Absorption spectra of solid para- and normal hydrogen in the first overtone region

G. Varghese, R. D. G. Prasad,* and S. Paddi Reddy
Department of Physics, Memorial University of Newfoundland, St. John's, Newfoundland, Canada A1B 3X7
(Received 9 July 1986)

Solid hydrogen crystals of both para and normal species were grown in a glass cell 6.4 cm long and 1.0 cm in diameter using liquid-helium cryogenics apparatus. Their infrared-absorption spectra were recorded in the first overtone region 8000—9400 cm^{-1}. The absolute intensities of several zero-phonon transitions of the type $Q_2(J)$, $Q_1(J)+Q_1(J)$, $S_2(J)$, $Q_2(J)+S_0(J)$, $Q_1(J)+S_1(J)$, $S_2(J)+S_0(J)$, and $S_1(J)+S_1(J)$ and those of the accompanying phonon branches Q_R and S_R were measured. The observed spectra clearly demonstrate that there is no contribution to the intensity of the pure overtone Q_R phonon branch from isotropic electron overlap induction mechanism. This is in striking contrast to the observations in the fundamental band of either solid [H. P. Gush, W. F. J. Hare, E. J. Allin, and H. L. Welsh, Can. J. Phys. 38, 176 (1960)] or gaseous [S. P. Reddy, G. Varghese, and R. D. G. Prasad, Phys. Rev. A 15, 975 (1977)] hydrogen.

I. INTRODUCTION

Solid hydrogen is unique among the molecular crystals because it retains almost free molecular rotation and free molecular vibration and exhibits many properties of a quantum crystal as revealed by several experimental studies both in Raman scattering[1,2] and infrared absorption.[3–6] In addition, the vibrational and rotational quantum numbers are good quantum numbers in the solid phase of H_2 because the mixing of states belonging to different values of v and J is negligible. In principle one can carry out experimental studies of pure solid para-H_2 ($J=0$), pure solid ortho-H_2 ($J=1$), or solid H_2 with any desired ortho-para mixture in order to understand various interactions and effects the solid H_2 crystals exhibit.

Since the first observation of the fundamental absorption of solid H_2,[7] there have been several studies of this absorption under different experimental conditions.[3–6] As in the case of gaseous H_2,[8] the observed absorption of solid H_2 in the fundamental region is due to the electric dipole moments induced by the intermolecular interaction. The observed spectral features of the $Q(\Delta J=0)$, $S(\Delta J=2)$, and $U(\Delta J=4)$ branches are briefly explained in the following manner: The relatively sharp zero-phonon transitions which involve only the internal degrees of freedom of the molecules are due to quadrupolar or hexadecapolar interaction. In the quadrupolar-induction mechanism, pertaining to the fundamental band, the isotropic polarizability of the interacting molecules gives rise to the zero-phonon transitions $Q_1(J)+Q_0(J)$ [or simply $Q_1(J)$], $S_1(J)+Q_0(J)$ [or simply $S_1(J)$], and $Q_1(J)+S_0(J)$;[9] the anisotropic component of the polarizability contributes exclusively to the zero-phonon transitions of the form $S_1(J)+S_0(J)$.[10] In the hexadecapolar-induction mechanism, the isotropic part of the polarizability of the interacting molecules contributes to the intensity of the zero-phonon $U_1(J)$ transitions.[4] The phonon branches which occur as sidebands on the higher-wave-number side of the zero-phonon transitions are due to the electron overlap interaction. In the fundamental band of solid H_2, the isotropic part of the overlap interaction contributes to the intensity of the phonon branch Q_R and the anisotropic part of the overlap interaction contributes to the phonon branches $S_R(J)$ and $U_R(J)$ and partly to $Q_R(J)$. The sideband phonon spectra result from transitions in which changes in the vibrational and rotational states are accompanied by a change in the state of lattice vibrations. The relative translational motion of the colliding pairs of H_2 molecules in gaseous phase corresponds to the lattice vibrations of H_2 in a crystal. In Fig. 1 we reproduce the fundamental band of solid normal H_2 in the region 4000—5300 cm^{-1} at 11.5 K reported by Gush *et al.*[11] Weaker $U_1(J)$ and $U_R(J)$ transitions in the fundamental band of solid H_2 which were first observed in our laboratory are given in Ref. 4.

Absorption spectra of pure rotational transitions $S_0(0)$ (Refs. 12 and 13), $S_0(1)$ (Ref. 13), $U_0(0)$ (Ref. 5) and $U_0(1)$ (Ref. 5) and those of double transitions $S_0(0)+S_0(1)$ (Ref. 5) and $S_0(1)+S_0(1)$ (Ref. 5) and the accompanying phonon spectra have also been reported.

Relative to the extensive experimental work done on the fundamental band of solid H_2, the amount of work done on its first overtone region is rather limited. A preliminary observation of absorption of solid normal H_2 in the first overtone region was first reported by Allin *et al.*[14] More recently Patel *et al.*[15] reported three zero-phonon transitions of solid normal H_2 in the first overtone region using a pulsed-laser piezoelectric-transducer optoacoustic spectroscopy. Kuo *et al.*[16] using the same technique as in Ref. 15 reported the positions of the TO- and LO-phonon maxima relative to the zero-phonon transitions. Considerable theoretical work has been done on the zero-phonon branches of the fundamental and pure rotational bands of solid H_2.[17,18] Theory of the phonon branches of the rotational and fundamental bands has also been given.[19,18] However, very little theoretical work has been reported on the spectra of solid H_2 in its overtone regions.

In the present paper we report the results of an experimental study of the infrared spectra of almost pure solid para-H_2 (~99% para) and solid normal H_2 (25% para) at

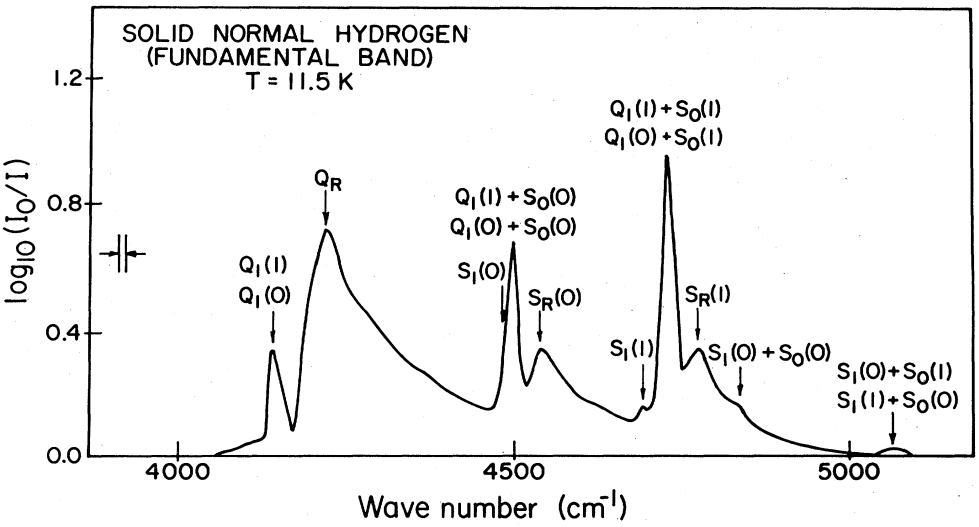

FIG. 1. An absorption profile of the fundamental band of solid normal H_2 at 11.5 K (adapted from Ref. 11).

~ 12 K in the first overtone region. The observed solid para-H_2 spectrum clearly demonstrates that the isotropic overlap induction mechanism does *not* contribute to the intensity of the pure overtone Q branch in contradistinction to that of the Q branch of the fundamental band. Zero-phonon transitions $Q_2(J)$, $Q_1(J)+Q_1(J)$, $S_2(J)$, $Q_1(J)+S_1(J)$, $Q_2(J)+S_0(J)$, $S_1(J)+S_1(J)$, and $S_2(J)+S_0(J)$ and the accompanying $Q_R(J)$ and $S_R(J)$ have been observed and their absolute absorption coefficients have been measured. Section II describes the experimental details. Results and discussion are presented in Sec. III.

II. EXPERIMENTAL DETAILS

A stainless-steel cryostat used for growing solid H_2 crystals was built to our specifications by the Janis Research Company, Inc. A schematic diagram of this cryostat is shown in Fig. 2. The main body of the cryostat, 75 cm long and 20 cm in diameter has a detachable tail piece. A steel tube 0.60 cm in diameter was provided in the center of the cryostat which extends into the tail section. A Pyrex glass cell 6.4 cm long and 1.0 cm in diameter was attached to the lower end of this steel tube by a Kovar seal. The cell has a jacket surrounding it, through which helium vapor was circulated to obtain the required low temperature. The flow of liquid helium through a capillary tube into this jacket can be controlled by a needle valve, located at the bottom of the helium dewar and operated from the top of the cryostat. Helium vapor from the jacket escapes through a capillary tube into the 2.5-cm-diameter stainless-steel tube surrounding the 0.6-cm tube in the center. The space between different chambers and the tail section were evacuated through the valve *H*. The outer dewar was precooled with liquid nitrogen before liquid helium was admitted into the helium dewar. During the precooling period the helium dewar was kept under a small positive pressure of helium gas.

Ultrahigh-purity normal hydrogen gas from Matheson was introduced into the cell through the central metallic tube in the cryostat. This tube was kept warm electrically to prevent solidification of H_2 inside it. Liquid helium was then introduced into the jacket around the cell through the capillary tube. Its rate of flow was adjusted by the needle valve. As the temperature of the cell was lowered, more hydrogen was admitted maintaining the pressure at about 3 psi. When the cell was filled with solid hydrogen, the heating coil wrapped on the outer jacket of the cell was activated to melt the solid; the helium flow was regulated such that the jacket contained only helium vapor, cold enough to condense hydrogen into a clear sample of solid. Once this stage was attained the solid remained clear for the entire period of the experiment.

For work on parahydrogen solid, gaseous parahydrogen was first produced by passing pure normal hydrogen through a column of the paramagnetic catalyst, APACHI-1 ($NiO{\cdot}2.5SiO_2$) (supplied by Houdry Process and Chemical Co.), kept inside a copper cylinder placed inside a separate helium dewar. Actually the copper cylinder was positioned in the helium dewar, just above liquid-helium level, such that the temperature of the cylinder was about 20 K. Hydrogen after passing through the catalyst at this low temperature was collected at the bottom of the cylinder in liquid form. The liquid was then allowed to vaporize by raising the copper cylinder inside the helium dewar and the evaporated gas was then admitted directly into the absorption cell. The procedure for growing parahydrogen crystals was similar to the one described for normal hydrogen crystals.

The source of radiation was a water-cooled General Electric FFJ quartzline projection lamp. The spectrometer used for recording the absorption spectra consisted of a Perkin Elmer Model G112 monochromator fitted with a 300 lines/mm reflection grating, a PbS detector, and a 260-Hz tuning fork chopper. The signal from the detector was amplified by a Dunn Model LI-101 preamplifier

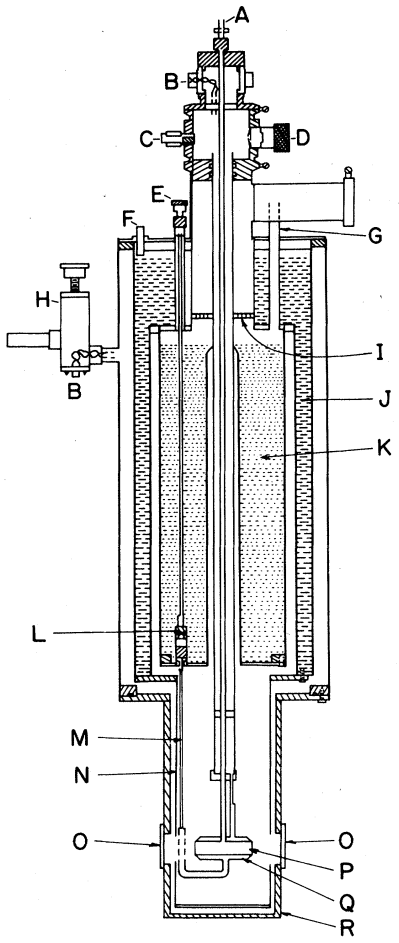

FIG. 2. Schematic diagram of the stainless steel liquid-helium dewar. *A*, Gas inlet; *B*, electrical feed through; *C*, safety pressure relief; *D*, vapor pumping post; *E*, helium needle valve control cap; *F*, liquid-nitrogen fill in the split cover (vent not shown); *G*, liquid-helium fill (vent not shown); *H*, evacuation valve; *I*, radiation baffle; *J*, liquid nitrogen; *K*, liquid helium; *L*, needle valve to adjust helium flow; *M*, capillary tube for helium flow; *N*, highly polished aluminum radiation shield; *O*, sapphire window; *P*, glass cell; *Q*, jacket of the glass cell; *R*, tail section of dewar.

and a Brower Laboratories Model 101 Lock-in voltmeter and then recorded on a Hewlett-Packard Model 7132A strip chart recorder.

The spectral region was calibrated using different orders of mercury emission lines.[20] Corning glass filter CS7-757 was used at the entrance slit of the spectrometer to eliminate the unwanted radiation. The slit width maintained at 50 μm gave a spectral resolution of 4.5 cm^{-1} at 8600 cm^{-1}.

III. RESULTS

Parahydrogen concentration was determined from the ratio R of the integrated absorption coefficient of $Q_1(0)+S_1(0)$ to that of $Q_1(0)+S_1(1)$ in the solid parahydrogen spectrum using the relation $R=(\frac{5}{3})C/(1-C)$ where C is the para concentration.[21] The integrated intensities $\tilde{\alpha}$ of the observed sharp zero-phonon and broad sideband phonon transitions were estimated by measuring the areas under the profiles and using the relation

$$\tilde{\alpha}=(c/Nl)\int \nu^{-1}\ln[I_0(\nu)/I(\nu)]d\nu\ ,$$

where c is the speed of light, N is the number of hydrogen molecules per cm^3 (2.609×10^{22} cm^{-3}), l is the length of the absorption sample, ν is the wave number in cm^{-1}, $I_0(\nu)$ is the intensity of the radiation incident on the sample, and $I(\nu)$ is the transmitted intensity. For the strong transitions the error in the estimated absorption coefficients is less than 5% and it is more for the weaker transitions.

A. Spectrum of solid para-H_2

Solid para-H_2 has only the $J=0$ level populated in its ground vibrational state. As a result one would expect a simpler spectrum with only three zero-phonon double transitions [$Q_2(0)+S_0(0)$, $Q_1(0)+S_1(0)$, and $S_1(0)+S_1(0)$] which are well separated. However, in the presence of even a small impurity of orthohydrogen a few more weak transitions are possible as seen from Fig. 3 which shows the spectrum of solid para-H_2 (99% para) at $\sim$12 K in its first overtone region 8000—9000 cm^{-1}.

The assignments of the transitions, the measured positions of their maxima and the corresponding $\tilde{\alpha}$ for solid parahydrogen are summarized in Table I. For comparison the wave numbers of the corresponding transitions in the gaseous phase calculated from the free molecular constants of H_2 (Ref. 22) are also included in the same table. The calculated wave numbers of the transitions in the spectrum of solid H_2 using the known Raman[1] and infrared[11] frequencies in the fundamental band of solid H_2 and the rotational constants of the ground vibrational level of the low-pressure H_2 gas,[22] (see, for example, Ref. (4)], are also given in Table I. The agreement between the measured and the calculated wavenumbers for the solid H_2 is within the experimental accuracy.

1. Pure vibrational transition $Q_2(0)$

Strictly speaking, this zero-phonon transition is forbidden in 100% pure parahydrogen. However, in the presence of ortho impurity this transition may appear as the double transition $Q_2(0)+Q_0(1)$ in which an ortho molecule undergoes an orientational transition. It is clear from the very weak intensity of this transition with no observable phonon sideband that the isotropic overlap contribution to the pure first overtone Q branch is absent. In contrast, in the fundamental band of solid 100% para-H_2 (Ref. 23) and of normal solid H_2 (Ref. 11) (see Fig. 1), the Q_R phonon sideband is the most intense one in the spectrum which is produced by the isotropic overlap interaction. This striking difference in these two spectra implies that the square of the matrix element of the induced isotropic overlap dipole moment $\langle v=0\,|\,\mu_{\text{overlap}}\,|\,v'=1\rangle^2$, which is a measure of the intensity of absorption

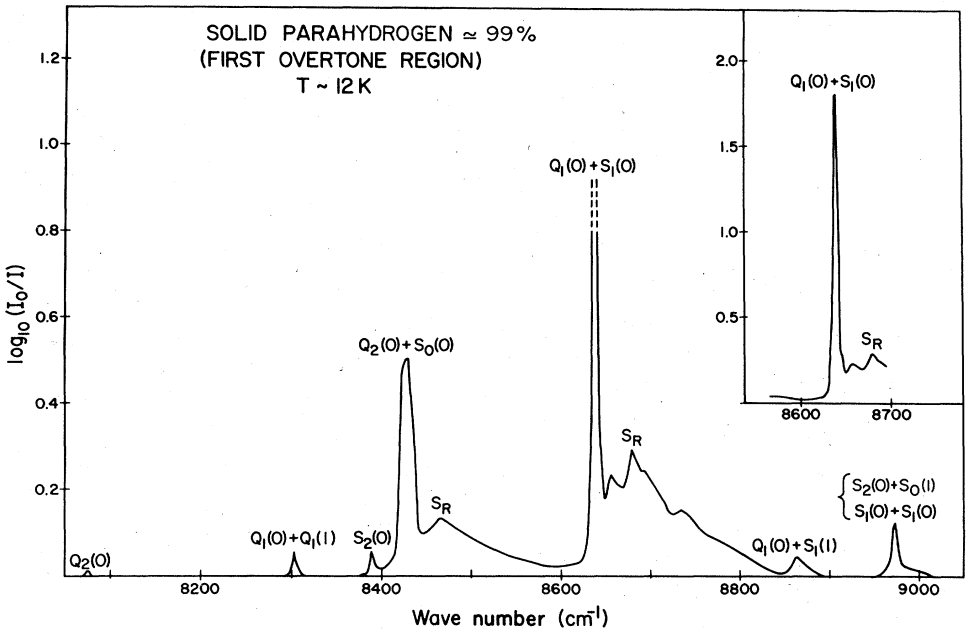

FIG. 3. Absorption profile of solid para-H_2 at ~ 12 K in the first overtone region with a sample path length of 6.4 cm.

of the phonon branch Q_R in the fundamental band, is large whereas the corresponding quantity $\langle v=0 \mid \mu_{\text{overlap}} \mid v'=2 \rangle^2$ is zero for the first overtone band.

2. *Double vibrational transition $Q_1(0)+Q_1(1)$*

The occurrence of this zero-phonon double vibrational transition in solid parahydrogen is possible because of the ortho impurity in the sample. One should note that the double transition $Q_1(0) + Q_1(0)$ is forbidden.

3. *Single transition $S_2(0)$*

This so-called zero-phonon single transition is actually $S_2(0) + Q_0(J)$. In the gaseous phase this transition is very strong,[24] whereas in the solid phase it is rather weak as seen in Fig. 3. The extremely weak intensity of this line is interpreted (see for example, van Kranendonk[25]) as a cancellation effect in an hcp lattice where the contributions from the first two neighboring shells to the coupling constant in the crystal field interaction vanishes and the contributions from the remaining shells are small. This zero

TABLE I. Wave-numbers and integrated absorption coefficients ($\tilde{\alpha}$) of various transitions of solid para-H_2 in the first overtone region at ~ 12 K.[a]

Transition	Measured wave number[b] (cm^{-1})	$\tilde{\alpha}$ (10^{-16} $cm^3 s^{-1}$)	Calculated wave number (cm^{-1}) Solid phase	Gas phase[c]
$Q_2(0)+Q_0(1)$	8075		8074.0	8087.0
$Q_1(0)+Q_1(1)$	8303	0.14	8299.2	8316.4
$S_2(0)$	8390	0.23	8390.0	8406.4
$Q_2(0)+S_0(0)$	8428	4.90	8429.4	8441.4
S_R	8468	5.60		
$Q_1(0)+S_1(0)$[d]	8640	7.20	8635.7	8659.0
S_R	8680	12.10		
$Q_1(0)+S_1(1)$	8857	0.23	8852.5	8874.0
$S_1(0)+S_1(0)$	8973	0.46	8971.7	8995.7
$S_2(0)+S_0(1)$			8976.8	8993.4

[a]Transitions involving $J=1$ occur because of small impurity of orthomolecules in the sample.
[b]The uncertainty in the measured wave numbers is ± 2 cm^{-1} except for the phonon maxima for which it is ± 10 cm^{-1}.
[c]Reference 22.
[d]The measured value in Ref. 26 is 8643 cm^{-1}.

contribution from the first two shells is not due to symmetry reasons but due to the accidental equality of the intermolecular separations of all the nearest neighbors.

4. *Vibration-rotation double transitions*

The zero-phonon double transitions $Q_2(0)+S_0(0)$ is a pure overtone one in which one molecule changes its v by 2 units and the other molecule makes a pure rotational transition. The full width at half maximum (FWHM) of this line is ~ 17 cm^{-1} which is rather large compared to other transitions in the para-H_2 spectrum. This is possibly due to the broader vibrational energy band in the $v=2$ state. The $Q_1(0)+S_1(0)$ transition is the strongest of all the transitions and its FWHM is ~ 5 cm^{-1} which compares with the spectral resolution of 4.5 cm^{-1} of the spectrometer used. The transition $Q_1(0)+S_1(1)$ is present because of the ortho impurity in the sample.

5. *Double S transitions $S_2(0)+S_1(0)$ and $S_1(0)+S_1(0)$*

The first of these transitions appears because of the ortho impurity. These transitions arise from the anisotropic polarizability in the quadrupolar induction mechanism.

6. *The phonon branches S_R*

The strong $Q_2(0)+S_0(0)$ and $Q_1(0)+S_1(0)$ zero-phonon transitions are accompanied by the broader phonon sidebands with clear maxima (see Fig. 3). The S_R branch accompanying $Q_1(0)+S_1(0)$ shows clearly four peaks. High-resolution work on solid para-H_2 is expected to reveal the nature of this structure.

B. The spectrum of solid normal H_2

In solid normal H_2 as both $J=0$ and 1 levels are populated one expects a richer spectrum in its first overtone region. Figure 4 shows the spectrum of solid normal H_2 at ~ 12 K in its first overtone region 8000—9400 cm^{-1}. The features of this spectrum are described in the following paragraphs.

The assignments of the transitions, the measured wave numbers of their maxima, and their absorption coefficients are given in Table II. The calculated wave numbers of these transitions in the solid and gaseous phases are also given in Table II. For comparison wave numbers for the transitions reported by Kuo *et al.*[26] are also included in the same table.

1. *Pure overtone zero-phonon Q lines and phonon Q branches*

On comparing Figs. 1 and 4 it is interesting to notice the striking difference between the Q branch of the fundamental band and that of the pure first overtone band. In Fig. 4 the pure overtone Q branch consists of two zero-phonon peaks, $Q_2(1)$ and $Q_2(0)$ with a separation of 12 cm^{-1}. A cursory inspection of Figs. 1 and 4 reveals that phonon Q_R branch in the fundamental band is much stronger than the zero-phonon Q line whereas the Q_R branch accompanying the $Q_2(J)$ transitions in the first overtone band is relatively weak. If one compares the integrated intensities of the phonon Q_R branch and the zero-phonon Q branch it is found that in the fundamental band the ratio of the integrated absorption coefficient of Q_R to that of $Q_1(J)$ is 12, whereas the corresponding ratio is only 1.5 in the first overtone band. This striking difference between the two bands can be explained in the following manner. In the fundamental band of solid H_2 the Q_R phonon arises mainly from the isotropic overlap interaction and only a small fraction of its intensity comes from the anisotropic overlap interaction. In the case of the first overtone band the isotropic overlap interaction vanishes and the only contribution to the phonon branch comes from the anisotropic overlap interaction. In the induced fundamental band of H_2 in the gas phase, the isotropic overlap, the anisotropic overlap, and the quadrupole induced components are identified with the coefficients B_{10}, B_{12}, and B_{32}, respectively.[27]

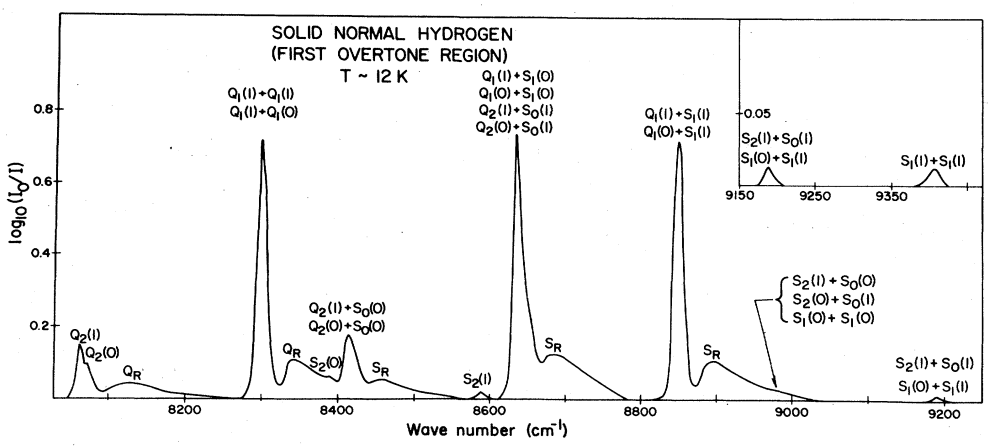

FIG. 4. Absorption profile of solid normal H_2 at ~ 12 K in the first overtone region with a sample path length of 6.4 cm.

TABLE II. Wave numbers and integrated absorption coefficients ($\tilde{\alpha}$) of various transitions of solid normal H_2 in the first overtone region at ~ 12 K.

Transition	Present work: Measured wave number[a] (cm^{-1})	Present work: $\tilde{\alpha}$ (10^{-16} $cm^3 s^{-1}$)	Kuo *et al.*[b]: Measured wave number (cm^{-1})	Calculated wave number (cm^{-1}): Solid phase	Calculated wave number (cm^{-1}): Gas phase[c]
$Q_2(1)+Q_0(0,1)$	8063	1.40		8063.1	8075.3
$Q_2(0)+Q_0(1)$	8075		8076	8074.0	8087.0
Q_R	8130	2.10			
$Q_1(1)+Q_1(1)$	8298	5.70	8304	8286.8	8310.4
$Q_1(1)+Q_1(0)$				8295.2	8316.4
Q_R	8340	3.20			
$S_2(0)$	8390			8390.0	8406.4
$Q_2(1)+S_0(0)$	8413	2.10		8416.5	8429.7
$Q_2(0)+S_0(0)$				8427.5	8441.4
S_R	8457	1.80			
$S_2(1)$	8590	0.07	8598	8589.0	8604.2
$Q_1(1)+S_1(0)$				8629.9	8653.1
$Q_1(0)+S_1(0)$	8635	6.50		8638.8	8659.0
$Q_2(1)+S_0(1)$				8651.2	8662.3
$Q_2(0)+S_0(1)$				8662.2	8674.0
S_R	8685	4.60			
$Q_1(1)+S_1(1)$	8850	5.20	8857	8846.4	8868.2
$Q_1(0)+S_1(1)$				8854.8	8874.1
S_R	8893	3.40			
$S_2(1)+S_0(0)$				8944.4	8958.6
$S_2(0)+S_0(1)$	8977			8977.0	8993.4
$S_1(0)+S_1(0)$				8975.9	8995.7
$S_2(1)+S_0(1)$	9189	0.15		9177.5	9191.2
$S_1(0)+S_1(1)$				9191.0	9210.7
$S_1(1)+S_1(1)$	9407	0.13		9406.0	9425.8

[a]The uncertainty in the measured wave numbers is ± 2 cm^{-1} except for the phonon maxima for which it is ± 10 cm^{-1}.
[b]Reference 26.
[c]Reference 22.

2. *Strong zero-phonon double transitions $Q_1(1)+Q_1(J)$, $Q_2(J)+S_0(0)$ and $Q_2(J)+S_0(1)$, and $Q_1(J)+S_1(1)$*

These three transitions are the strongest in the spectrum and have approximately the same intensity maxima. The half-widths (FWHM) of these lines are 15 cm^{-1}, 17 cm^{-1}, and 15 cm^{-1}, respectively. The $Q_2(J)+S_0(0)$ transition is not as intense as compared to the same transitions in solid para-H_2. But its width is comparable to that of $Q_2(0)+S_0(0)$ in solid para-H_2 which is 24 cm^{-1}. The four zero-phonon transitions are accompanied on the higher wave-number side by the usual broad phonon sidebands whose measured peak positions are also listed in Table II.

TABLE III. Separations between the phonon branch maxima and the corresponding zero-phonon maxima.

Assignment	Separation (cm^{-1})
Parahydrogen	
$S_R-[Q_2(0)+S_0(0)]$	40
$S_R-[Q_1(0)+S_1(0)]$	40
Normal hydrogen	
$Q_R-[Q_2(J)]$	55
$Q_R-[Q_1(1)+Q_1(J)]$	42
$S_R-[Q_2(J)+S_0(0)]$	44
$S_R-\begin{bmatrix}Q_1(J)+S_1(0)\\ Q_2(J)+S_0(1)\end{bmatrix}$	50
$S_R-[Q_1(J)+S_1(1)]$	43

3. *Single transitions $S_2(0)$ and $S_2(1)$*

These transitions are very weak. The reason for the weak intensity of these transitions is the same as given for $S_2(0)$ in para-H_2. Three peaks corresponding to transitions of the type $S_2(J)+S_0(J)$ and $S_1(J)+S_1(J)$ are observed at 8977 cm^{-1}, 9189 cm^{-1}, and 9407 cm^{-1} and their actual assignments are given in Table II.

In Table III we present the separations between the maxima of the zero-phonon transitions and the maxima of the corresponding sideband phonon branches for the various transitions observed in both solid para-H_2 and solid normal H_2. These values are in the range 40—55 cm^{-1}.

IV. CONCLUDING REMARKS

In this paper we have reported the findings of our experiments with solid para- and normal H_2 in its first overtone region. A comparison of our observations with the available data for the fundamental band of solid H_2, both in the para state and normal state, clearly indicates that the isotropic overlap interaction which gives rise to 90% of the intensity of the pure vibrational band in the fundamental band is absent in its first overtone pure vibrational band for solid parahydrogen. In the case of solid normal hydrogen, the only part which contributes to the phonon branch in the pure first overtone vibrational band is the anisotropic overlap interaction which is relatively weak. It is also evident that the intensity of the phonon branches arising from the anisotropic overlap interaction is dependent on the intensity of the associated zero-phonon branches. On the other hand the intensity of the phonon branches arising from the isotropic overlap interaction is independent of the intensity of the corresponding zero-phonon transitions. The small values of absorption coefficients of the single transitions $S_2(0)$ and $S_2(1)$ are explained as due to a cancellation effect. Experiments with higher resolution are expected to reveal some of the unresolved features of the spectra.

ACKNOWLEDGMENT

This research was supported in part by a grant awarded to S.P.R. from the Natural Sciences and Engineering Research Council of Canada. The authors acknowledge with pleasure the assistance of T. G. White in preparing the apparatus for the experiment.

---

*Present address: Department of Physics, Ranchi University, Ranchi, Bihar, India.

[1]See for example, S. S. Bhatnagar, E. J. Allin, and H. L. Welsh, Can. J. Phys. **40**, 9 (1962).

[2]See for example, P. A. Fleury and J. P. McTague, Phys. Rev. A **12**, 317 (1975).

[3]See for example, S. I. Boggs, M. J. Clouter, and H. L. Welsh, Can. J. Phys. **50**, 263 (1972), and the references therein.

[4]R. D. G. Prasad, M. J. Clouter, and S. P. Reddy, Phys. Rev. A **17**, 1690 (1978).

[5]T. K. Balasubramanian, Chen-Hsin Lien, J. R. Gains, K. Narahari Rao, and E. K. Damon, J. Mol. Spectrosc. **92**, 77 (1982).

[6]M. Jean-Louis, M. M. Thiery, H. Vu, and B. Vodar, J. Chem. Phys. **55**, 4657 (1971); M. Jean-Louis and H. Vu, Rev. Phys. Appl. **7**, 89 (1972).

[7]E. J. Allin, W. F. J. Hare, and R. E. MacDonald, Phys. Rev. Lett. **9**, 554 (1955).

[8]See S. P. Reddy, in *Phenomena Induced by Intermolecular Interaction,* edited by G. Birnbaum (Plenum, New York, 1985).

[9]The rotational quantum number J is 0 or 1 for solid H_2 and the subscripts 0, 1, and 2 refer to the change in the vibrational quantum number v from 0. In particular, $Q_0(J)$ represents an orientational transition with no change in J.

[10]A. Sen, R. D. G. Prasad, and S. P. Reddy, J. Chem. Phys. **72**, 1716 (1980).

[11]H. P. Gush, W. F. J. Hare, E. J. Allin, and H. L. Welsh, Can. J. Phys. **38**, 176 (1960).

[12]M. Trefler, M. Cappel, and H. P. Gush, Can. J. Phys. **47**, 215 (1969).

[13]U. Buontempo, S. Cunsolo, P. Dore, and L. Nencini, Can. J. Phys. **60**, 1422 (1982).

[14]E. J. Allin, H. P. Gush, W. F. J. Hare, J. L. Hunt, and H. L. Welsh, Colloq. Int. C.N.R.S. **77**, 21 (1957).

[15]C. K. N. Patel, E. T. Nelson, and R. J. Kerl, Phys. Rev. Lett. **47**, 1631 (1981).

[16]C. Y. Kuo, N. M. F. Vieira, and C. K. N. Patel, Phys. Rev. Lett. **49**, 1284 (1982).

[17]J. Van Kranendonk and G. Karl, Rev. Mod. Phys. **40**, 531 (1968), and the references therein.

[18]J. D. Poll and R. H. Tipping, Can. J. Phys. **56**, 1165 (1978).

[19]J. D. Poll and J. Van Kranendonk, Can. J. Phys. **40**, 163 (1961).

[20]*IUPC Tables of Wave numbers for Calibration of Infrared Spectrometers,* 2nd ed., edited by A. R. H. Cole (Pergamon, Oxford, 1977).

[21]I. F. Silvera, W. N. Hardy, and J. P. McTague, Discuss. Faraday Soc. **48**, 54 (1970).

[22]J. V. Foltz, D. H. Rank, and T. A. Wiggins, J. Mol. Spectrosc. **21**, 203 (1966).

[23]W. F. J. Hare, E. J. Allin, and H. L. Welsh, Phys. Rev. **99**, 1887 (1955).

[24]S. P. Reddy, E. van Nostrand, and P. G. Gillard (unpublished).

[25]J. Van Kranendonk, *Solid Hydrogen* (Plenum, New York, 1983), pp. 88–91.

[26]C. Y. Kuo, R. J. Kerl, N. D. Patel, and C. K. N. Patel, Phys. Rev. Lett. **53**, 2575 (1984).

[27]J. D. Poll, J. L. Hunt, and J. W. MacTaggart, Can. J. Phys. **53**, 954 (1975).